# Three-Dimensional Hard Dumbbell Solid Free Energy Calculation Via the Fluctuating Cell Model

Steven A. Kadlec
*Physical and Chemical Properties Division, MC: 838.08, National Institute of Standards and Technology, 325 Broadway, Boulder, Colorado 80305 and Department of Physics, University of Colorado at Boulder, Box 390, Boulder, Colorado 80309*

Paul D. Beale
*Department of Physics, University of Colorado at Boulder, Box 390, Boulder, Colorado 80309*

James C. Rainwater
*Physical and Chemical Properties Division, MC: 838.08, National Institute of Standards and Technology, 325 Broadway, Boulder, Colorado 80305*

Abstract:

Determination of the solid-liquid phase transition point of a molecular substance requires calculation of the free energy in both phases. Progress has been made on this problem by modeling molecules as fused hard spheres and adding attraction and electric multipole moments perturbatively. The solid free energy of hard heteronuclear dumbbells of bond length $L^*$, used to model diatomic molecules, can in principle be calculated exactly via the Frenkel-Ladd method, but this is computationally intensive. Use of Lennard Jones-Devonshire fixed cells to calculate free energy is much simpler computationally but is an approximation. The fluctuating cell model is investigated as an alternate intermediate method which is still computationally simpler than Frenkel-Ladd. As was found earlier in two dimensions, for small $L^*$ the simple cell model is in better agreement with Frenkel-Ladd than the fluctuating cell model, but for larger $L^*$ the fluctuating cell model is in better agreement. The probability distributions of free volumes are also analyzed and show different functional behavior for near-zero bond length and appreciable bond length.

Introduction:

The determination of the solid-liquid phase transition is of considerable current interest. Monson et al. have reviewed various methods available for solid-liquid equilibrium calculations [1]. These methods detail the calculation of the free energy in both the solid and liquid phases as this is required to determine the phase transition. Some models ignore intermolecular forces focusing on hard infinitely repulsive forces characterized solely by the molecule's shape and size. One question these models try to answer is how much physics can be realized by considering only the molecular form. The hard sphere model, for example, helps reveal the basic physics involved in the freezing of inert gasses. Hard heteronuclear dumbbell models have helped explain the freezing of methyl chloride [2]. Hard chain molecules have provided insight into the freezing of n-alkanes [3]. These hard models can serve as the foundation to interactions that are more complicated. Such interactions as dipole moments and Van der Waals attraction can be added perturbatively.

There are a number of methods for calculating the free energy of these hard models. In theory, thermodynamic integration can generate exact free energies. This method, however, is limited by long computation times. The simple cell method of Lennard-Jones and Devonshire approximates the free energy through calculation of the free volume available to a single particle in a cage (or cell) of nearby particles each fixed to its respective lattice site [1]. This method leads to a first order approximation of the free energy. The free volume is defined by

$$v_f = \int_{cell} d\vec{r} e^{-\beta U(\vec{r},\vec{r}_1,\ldots,\vec{r}_Q)} \tag{1}$$

where Q is the number of nearest neighbors that form the cell. In the case of hard interactions, the Boltzman factor reduces simply to zero at the edge of the cell and evaluates to one within the cell's boundary walls. The reduced free energy can then be approximated by $f \approx -\ln\left(v_f / l^D\right)$ where $l$ is an arbitrary length scale and $D$ is the dimensionality of the system.

A natural extension of the simple cell method makes use of an equilibrated system of hard particles in the solid state. This fluctuating cell theory requires calculating and then averaging the free volume $v_f$ of many particles of the system. The reduced free energy is then calculated as $f \approx -\ln\left\langle v_f / l^D \right\rangle$. It should be noted that the work of Hoover et al. [4] included an alternate expression for the free energy, $f_{alt} \approx -\left\langle \ln\left(v_f / l^D\right)\right\rangle$. However, the former expression was determined to better approximate the free energy.

A two-dimensional system of hard dumbbells was studied by Gay et al. [5]. Their work indicates that the fluctuating cell theory produces good free energy approximations for this system. At near zero $L^*$ the simple cell method actually performs better, but as the bond length is increased, the fluctuating cell theory outperforms the simple cell. They also determined that the functional form of the free volume distribution is markedly different for a system of near zero $L^*$ dumbbells and those of larger $L^*$. The small bond length systems have free volume distributions that peak at $v_f = 0$ while the elongated dumbbells have free volume distributions that peak at some non zero value.

One of us (J. C. R.) found an analytic solution to calculate the free volume of a three-dimensional system of hard spheres [6]. This solution was developed independently and concurrently with an analytic solution found by Sastry et al. [7]. The forms of the two solutions are quite different but they produce identical free volumes.

In a collaboration between M. Lusk and one of us (P. D. B.) to calculate the interfacial free energy of grain boundaries of steric assemblies of elastic disks, the fluctuation cell model proved beneficial [8]. Unlike other methods, it did not require an attractive potential and could be applied to a static snapshot of an equilibrated system. The free energy calculation required calibration with the simple cell method on a homonogenous system of disks.

Method:

A Monte Carlo simulation was performed on a system of three-dimensional hard homonuclear dumbbells (figure 1) in the NVT ensemble. The system was initiated in the CP1 solid phase with the number of particles being 6x6x4 in each of the three lattice directions. The correct number density was imposed by scaling the lattice vectors of the close packed CP1 solid. Periodic boundary conditions were employed. Once equilibrated, the free volume of each particle was calculated. Free energies were derived from the average of the free volume.

CP1 crystal details:

The CP1 crystal structure was first introduced by Vega et al. [9]; however, written details of the structure are lacking. An intuitive means for visualizing the close packed CP1 structure is as follows: 1) Label the two spheres A and B of each dumbbell. 2) Orient all particles in the same direction. 3) Make a close packed triangular lattice of mxn particles out of sphere A of the dumbbells. This defines the $\vec{a}_1$ and $\vec{a}_2$ lattice vectors. 4) Rotate all particles about the center of sphere A such that sphere B of each dumbbell touches sphere A of two of the dumbbells below. Rotate all the dumbbells this way such

that they are all oriented in the same direction. All the B spheres now make a triangular close packed lattice. 5) Take another mxn dumbbells and place a triangular lattice of the A spheres on top of the B spheres of the lower lattice such that each A sphere touches three B sphere's and each B sphere touches three A spheres (except for edge dumbbells). 6) Orient the new dumbbells in the same direction as those below. The $\vec{a}_3$ lattice vector can be defined from the geometrical center of one of the lower dumbbells to the geometrical center of the upper adjacent dumbbell that is farthest away. Repeat steps 5 and 6 to build the solid. The alternations in sphere placement should be constructed such that as $L^*$ is reduced to zero, the solid would become an FCC close packed hard sphere system with the usual XYZXYZ sequence of planer triangular lattices. For this simulation, the solid was built only in the positive lattice vector directions measured from an arbitrary origin.

The bond length $L^*=L/\sigma$ defines the orientation of the dumbbells in the CP1 crystal where $\sigma$ is the diameter of one of the spheres of the hard dumbbell (Figure 1). Throughout the rest of this discussion, all lengths will be reduced by $\sigma$. The angle between $\vec{a}_3$ and the normal to the plane of $\vec{a}_1$ and $\vec{a}_2$ is $\psi = \sin^{-1}(L^*/\sqrt{3})$. Defining $a^*$ as the magnitude of the $\vec{a}_1$ and $\vec{a}_2$ lattice vectors, $a^*=|\vec{a}_1|/\sigma=|\vec{a}_2|/\sigma$, gives the magnitude of $\vec{a}_3$ as $a_3^* = |\vec{a}_3|/\sigma = Ra^*\sqrt{3+5L^{*2}+2\sqrt{2}L^*\sqrt{3-L^{*2}}}\,/\sqrt{3}$ where

$$R = \frac{a_3/a_1}{(a_3/a_1)_{cp}} \tag{2}$$

where $(a_3/a_1)_{cp}$ is the close packed ratio. An arbitrary density can be imposed by scaling the $\vec{a}_1$ and $\vec{a}_2$ lattice vectors of the close packed system by $a^*$ and by scaling the close packed $\vec{a}_3$ lattice vector by $Ra^*$. The relation between the nearest neighbor distance and density, $\rho^* = \rho d^3 = Nd^3/V$ is as follows:

$$a^*(\rho, L^*, R) = \left( \frac{2+3L^*-L^{*3}}{R\rho^*\left(\sqrt{2}+L^*\sqrt{3-L^{*2}}\right)} \right)^{1/3} \tag{3}$$

Here, d is the diameter of a sphere with the same volume as the dumbbell,

$$\frac{d}{\sigma} = \left(1+\frac{3}{2}L^*-\frac{L^{*3}}{2}\right)^{1/3} \tag{4}$$

It should be noted here that the expression for the close packed density as reported by Vega et al. [9] is in form quite different then the expression found for this paper. The close packed density used here is

$$\rho_{cp}^* = \frac{2+3L^*-L^{*3}}{\sqrt{2}+L^*\sqrt{3-L^{*2}}} \tag{5}$$

The form used by Vega et al. is much more complicated; however, computationally these two forms are equivalent. They produce identical close packed densities

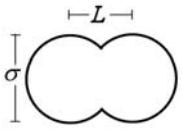


Figure 1. A single hard dumbbell with bond length, $L$.

In the simulation, cell lists were employed to limit the number of distance calculations required when determining particle overlap. It is important to ensure that the cells are not too small. If they are, two particles may overlap that are not in neighboring cells. The largest distance between two overlapping dumbbells is $L^*$+1. This must be the minimum distance between two parallel walls of the cell. The edges of the cells were along lattice vectors: $e_1$ along $\vec{a}_1$, $e_2$ along $\vec{a}_2$, etc. The minimum lengths of these edges $e_1, e_2$, and $e_3$ were determined:

$$e_1 = e_2 = \frac{\sqrt{9+14L^{*2}-3L^{*4}+8\sqrt{2}L^*\sqrt{3-L^{*2}}}\left(L^*+1\right)}{\sqrt{3}\left(\sqrt{2}+L^*\sqrt{3-L^{*2}}\right)} \tag{6}$$

$$e_3 = \frac{\sqrt{3+5L^{*2}+2\sqrt{2}L^*\sqrt{3-L^{*2}}}\left(L^*+1\right)}{\sqrt{2}+L^*\sqrt{3-L^{*2}}} \tag{7}$$

Space was divided into an integral number of cells in each of the three lattice vector directions such that each cell had the smallest edge lengths possible.

Trial Moves:

The Monte Carlo simulation required trial translational and orientation moves. The orientation of each dumbbell was tracked by a unit vector ($\hat{v}_i, i=1,..,N$) connecting the centers of the spheres of the dumbbell. 5000 Monte Carlo steps were used to equilibrate the system, and 20 independent systems were generated for each free energy calculation. The translational and orientation step sizes were adjusted to allow for a roughly 50% acceptance rate of each trial move.

Translations were performed by randomly choosing a displacement along each of the lattice vector directions. In addition, positions of each particle were tracked in the lattice vector coordinate system. Before any distance calculations were performed, displacement vectors were transformed to a Cartesian coordinate system. The x-axis was aligned along $\vec{a}_1$, and the xy plane was positioned in the $\vec{a}_1\,\vec{a}_2$ plane. In Cartesian coordinates

$$\vec{a}_1^* = a^*\left[1,0,0\right],\ \vec{a}_2^* = a^*\left[\frac{1}{2},\frac{\sqrt{3}}{2},0\right], \tag{8),(9}$$

$$\text{and } \vec{a}_3^* = Ra^*\left[\frac{1}{2}(1+L^{*2}),\frac{1}{2\sqrt{3}}(1+L^{*2}),\frac{1}{\sqrt{3}}\left(\sqrt{2}+L^*\sqrt{3-L^{*2}}\right)\right]. \tag{10}$$

The transformation matrix is

$$\vec{r}_{CC} = \begin{bmatrix} 1 & 1/2 & \dfrac{\sqrt{3}(1+L^{*2})}{2\sqrt{3+5L^{*2}+2\sqrt{2}L^{*}\sqrt{3-L^{*2}}}} \\ 0 & \sqrt{3}/2 & \dfrac{(1+L^{*2})}{2\sqrt{3+5L^{*2}+2\sqrt{2}L^{*}\sqrt{3-L^{*2}}}} \\ 0 & 0 & \dfrac{\sqrt{2}+L^{*}\sqrt{3-L^{*2}}}{\sqrt{3+5L^{*2}+2\sqrt{2}L^{*}\sqrt{3-L^{*2}}}} \end{bmatrix} \vec{r}_{LVC}, \tag{11}$$

where $\vec{r}_{CC}$ is the position vector in Cartesian coordinates, and

$$\vec{r}_{LVC} = g\hat{a}_1 + h\hat{a}_2 + j\hat{a}_3 = \begin{bmatrix} g \\ h \\ j \end{bmatrix} \tag{12}$$

is the position vector in the lattice vector coordinate system. Note that all direction vectors are unit vectors.

Orientation trial moves were generated by picking a random unit 3-vector, $\hat{t}$. This vector was then shrunk by an amount, $\omega$ and added to the original orientation vector, $\hat{u}_i$. The new orientation vector was then normalized and given by

$$\hat{u}_i^{'} = \frac{\hat{u}_i + \omega\hat{t}}{\left|\hat{u}_i + \omega\hat{t}\right|}. \tag{13}$$

Free Energy Calculation:

Upon equilibration, the free volume of each particle was calculated via Monte Carlo integration. One dumbbell was selected and wandered randomly to determine the maximum box volume, $V_b$ within which to sample points. The minimum and maximum coordinates in all three of the lattice vector directions were recorded ($b_{i,min}$, $b_{i,max}$, $i$=1,2,3). Random orientations were chosen when the dumbbell hit another particle to determine if the range of motion could be extended by extreme variation in the orientation. After the edges of the integration space were determined, each edge ($b_{i,max} - b_{i,min}$) was increased by 10% about its center just to ensure that the entire free volume was contained within the box. When a large enough number of random walk steps are performed, the free volume becomes independent of the number of steps taken.

After the sample space was determined, a Monte Carlo integration was performed over three translational and two angular dimensions. The angular integration was performed by picking random unit vectors to specify the dumbbell's orientation. The number of accepted positions, $N_A$ was tracked out of the total number of trial positions, $N_T$. A free volume was calculated as $v_{f,i}^{*} = \frac{N_A}{N_T} V_b^{*}, i = 1,...,N$ where

$$V_B^* = \frac{\sqrt{6}+\sqrt{3}L^*\sqrt{3-L^{*2}}}{2\sqrt{3+5L^{*2}+2\sqrt{2}L^*\sqrt{3-L^{*2}}}}\prod_{i=1}^{3}(b_{i,max}^* - b_{i,min}^*)\,. \quad (14)$$

The free volume of each particle was calculated in this manner. The free energy was approximated by $f^* = \frac{F}{Nk_BT} - \Pi = -\ln\left(\left\langle v_{f,i}^* \right\rangle\right)$ where $\Pi$ is the kinetic part of the free energy

$$\Pi = -\frac{1}{N}\ln\left\{\frac{\left(8\pi^2\sigma^3\right)^N}{h^{6N}}\int d\vec{p}_1...d\vec{p}_N e^{-\beta\sum_{i=1}^{N}\frac{\vec{p}_i^2}{2m}}\int d\vec{L}_1...d\vec{L}_N \exp\left[-\beta\sum_{i=1}^{N}\left(\frac{L_{x,i}^2+L_{y,i}^2}{2I_0}+\frac{L_{z,i}^2}{2I_1}\right)\right]\right\}, \quad (15)$$

where $I_1$ is the moment of inertia about the axis connecting the spheres of the dumbbell, and $I_0$ is the moment of inertia about the two axis perpendicular to this.

Results

Table 1 shows the results of the Vega et al. using the Frenkel-Ladd method. They are compared to the fluctuating cell and simple cell results. This table shows that at low values of $L^*$ the simple cell method does a better job at approximating the free energy. According to these results, if $L^* \geq 0.6$ then the fluctuating cell method approximates the free energy better. Note that the fluctuating cell method always produces free energies that are higher than those computed via thermodynamic integration. Conversely, the simple cell method always underestimates the free energy.

| $L^*$ | $R$ | $\rho^*$ | $f^*$ [9] (Vega) | $f^*$ (*fluct.*) | $f^*$ (*simp.*) | *% diff (fluct.)* | *% diff (simp.)* |
|---|---|---|---|---|---|---|---|
| 0.0 | 1.00 | 1.041 | 4.96 | 5.75(2) | 4.91492(6) | 15.9% | 0.909% |
| 0.3 | 0.94 | 1.235 | 9.96 | 10.73(3) | 9.5833(3) | 7.73% | 3.78% |
| 0.6 | 0.96 | 1.289 | 12.86 | 13.38(3) | 12.1141(7) | 4.04% | 5.80% |
| 1.0 | 0.96 | 1.18 | 13.34 | 13.74(3) | 12.595(1) | 3.00% | 5.58% |

Table 1. The numbers in parenthesis indicate the uncertainty in the last digit printed. The last two columns show the percent difference of the fluctuating and simple cell free energies with respect to the results of Vega et al.

In accordance with the work of Gay et al. [5], the effect of bond length on the free volume distribution was investigated. Figure 2 shows the distribution for small $L^*$. Here it is clear that the probability of having zero free volume is tending toward zero although there is not enough evidence to state that the probability is exactly zero at zero free volume. There is a peak in the distribution at a nonzero free volume. As the bond length is increased, however, the orientation of the dumbbell plays a larger role in determining the free volume. Even at $L^*$=0.10 the probability of having a zero free volume tends to a large nonzero value (perhaps even a singularity). The peak in the distribution occurs at zero free volume (figure 3).

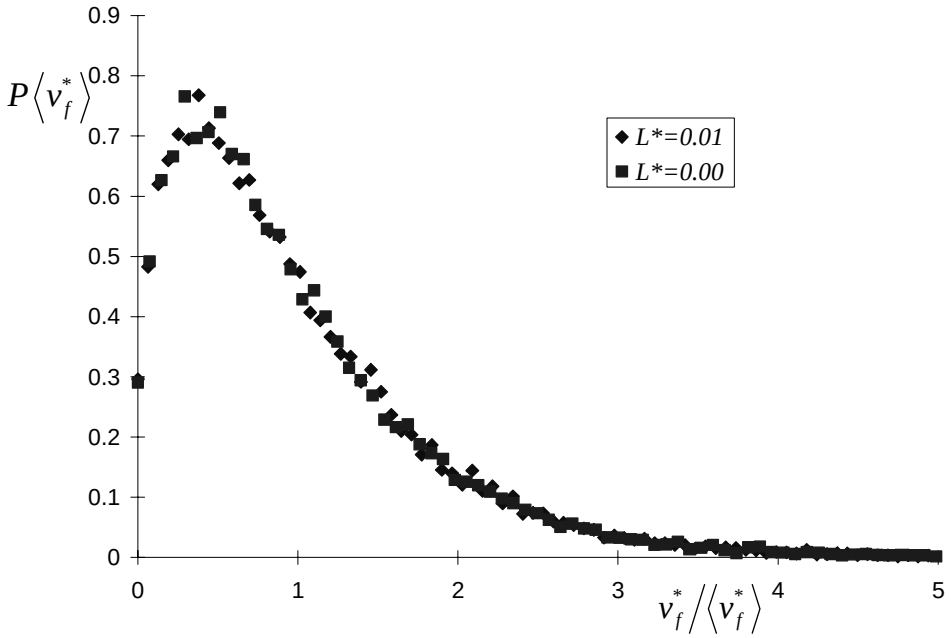


Figure 2. Free volume distribution for small $L^*$. Note that the probability of zero free volume tends toward zero. Here $\rho^* = 1.18$ and R=1.00.

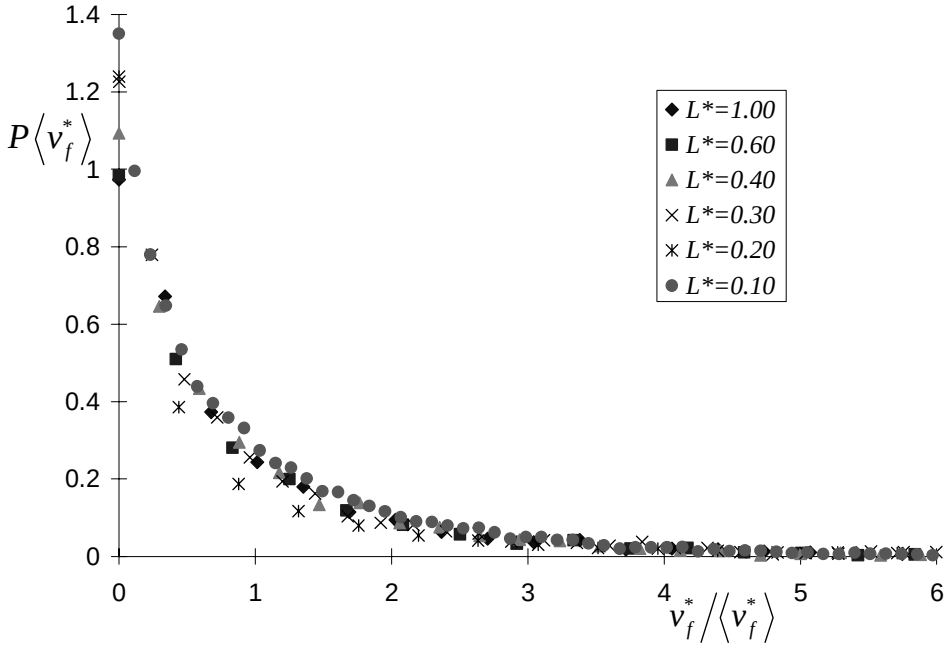


Figure 3. Here, the probability distribution peaks as the free volume approaches zero (perhaps a singularity). Again, $\rho^* = 1.18$ and R=1.00.

| $L^*$ | $\langle v_f^* \rangle$ |
|---|---|
| 0.00 | $6.20(4) \times 10^{-4}$ |
| 0.01 | $6.18(4) \times 10^{-4}$ |
| 0.10 | $3.43(3) \times 10^{-4}$ |
| 0.20 | $9.53(14) \times 10^{-5}$ |
| 0.30 | $5.12(13) \times 10^{-5}$ |
| 0.40 | $3.60(9) \times 10^{-5}$ |
| 0.60 | $1.56(4) \times 10^{-5}$ |
| 1.00 | $9.6(2) \times 10^{-7}$ |

Table 2. Average free volume at various bond length and constant $\rho^* = 1.18$ and $R$=1.00. The numbers in parenthesis give an estimate of the uncertainty in the last digit(s) printed.

In the hard sphere limit of $L^*$, the simple cell outperforms the fluctuating cell model; however, the fluctuating cell model may still have utility in free volume calculations even for these systems. For $L^*$=0, the difference between the simple cell and fluctuating cell free energies was determined and is plotted in figure 3. The free energy difference is nearly constant. This is because the fluctuating cell to simple cell free volume ratio is nearly independent of density. In fact, figure 4 shows that the free volume distribution is density independent. The fluctuating cell method could be used to determine the free energy if properly calibrated. When calculating the free energy of grain boundaries, this method would be preferable. Also, since most simulations require fluctuation of the system, a snapshot of the equilibrated system could lead to a fairly good free energy estimate simply by calculating the free volume.

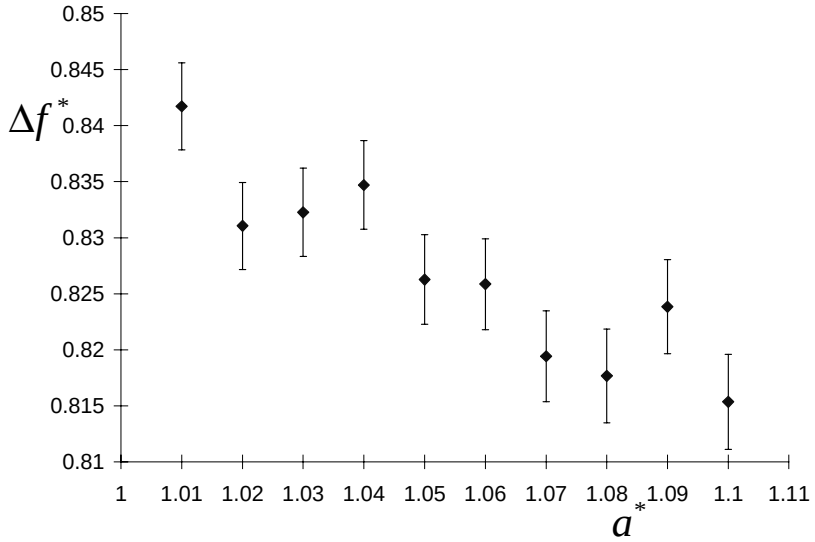


Figure 3. The difference between the fluctuating and simple cell free energies for the hard sphere system. The fluctuating cell free energy is always larger. Here, $L^*$=0.0 and $R$=1.00.

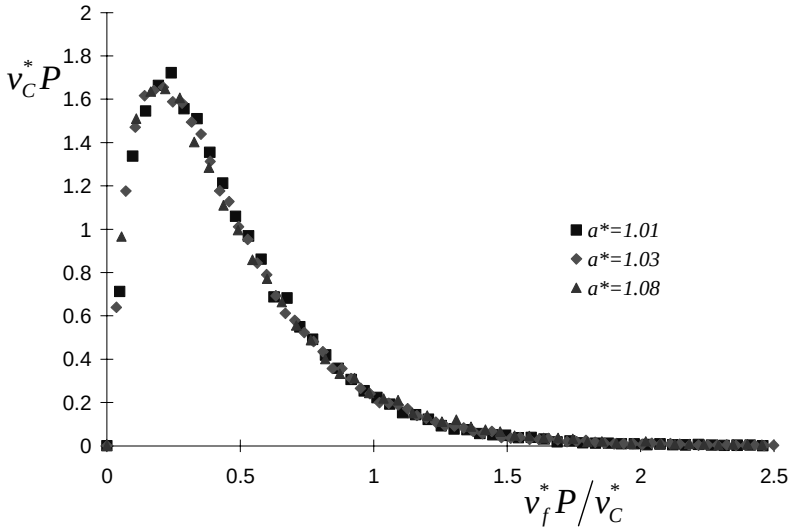


Figure 4. The hard sphere free volume distribution is independent of density. Here, $v_C^*$ is the simple cell free volume. Here, $L^*$=0.0 and $R$=1.00.

The results of the 3D fluctuating cell model are analogous to the fluctuating cell model applied to 2D homonuclear dumbbells. Gay et al. describes the same trend in the utility of the fluctuating cell model [5]. At zero $L^*$ the simple cell model proves more accurate than the fluctuating cell. As the bond length is increased, the fluctuating cell model better approximates the free energy. It was noted that the transition value of $L^*$ where the fluctuating cell model outperformed the simple cell model was larger in the three-dimensional case than in two-dimensions. Even at $L^*$=0.3, in three-dimensions, the simple cell was more accurate. In addition, the free volume distribution of the three-dimensional system has similar characteristics to that of the two-dimensional system. At some appreciable $L^*$ the distribution switches from peaking at some nonzero free volume to peaking at $v_f^* = 0$.

The simple cell free energy dependence on $L^*$ is also interesting. Near $L^*$=0, in both two [5] and three dimensions the free energy as calculated by the simple cell method decreases with increasing $L^*$ (Figure 5). At some small $L^*$, however, the trend is reversed as the free energy increases with increasing $L^*$. This is most likely due to the locking of the dumbbell's rotation as the bond length is increased. This decreases the orientations available and thus the total free volume. At small rotation, $L^*$ plays little role in the free volume as the solid is a plastic crystal. Note that the fluctuating cell model, however, gives free energies that are monotonically increasing for all $L^*$ values

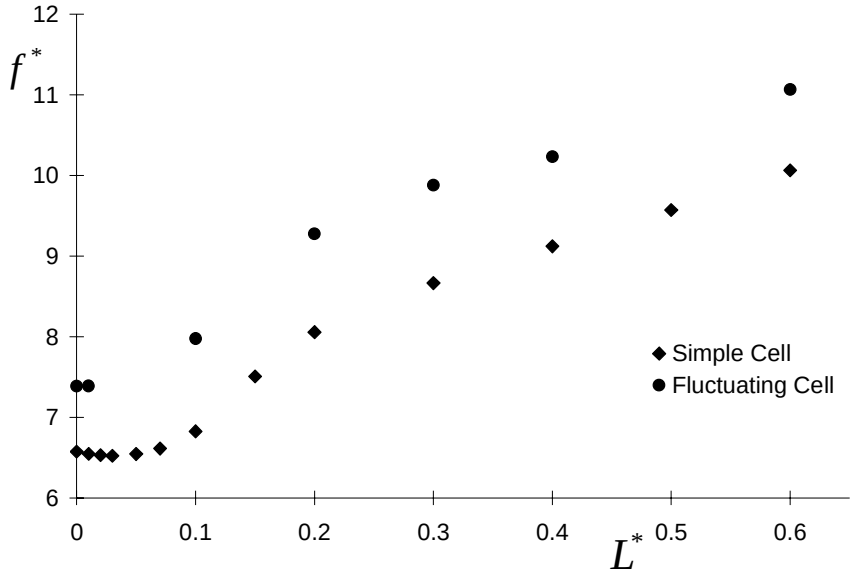


Figure 5. Comparison of the free energy as calculated by the fluctuating and simple cell models. $\rho^* = 1.18$, and $R$=1.00.

One of us (J. C. R.) derived an analytic solution for the free volume of a three-dimensional system of hard spheres [6] in agreement with an independent analytic solution of Sastry, et al. [7]. Shawn C. Gay coded this solution for the free volumes, and these results were compared with those found by Monte Carlo integration. Although the code for the analytic method either crashed or produced clearly incorrect results roughly 0.05% of the time, it usually agreed with Monte Carlo integration within the estimated uncertainty.

Conclusion:

From the free energy calculations via thermodynamic integration on the CP1 crystal, the simple cell approximates the free energy better only near the hard sphere limit. The real benefit of the fluctuating cell model lies in its ability to give thermodynamic information about a system from a single configuration. In addition, there appears to be improvement in the free energy calculation over the simple cell for dumbbells with appreciable elongation.

Acknowledgment:

We thank Shawn Gay for programming the analytical free volume calculation for the hard sphere system.

References:

[1] P. A. Monson and D. A. Kofke. Advances in Chemical Physics. **115**, 113 (2000).
[2] S. C. Gay, P. D. Beale, and J. C. Rainwater. Int. J. Thermophysics. **19,** (1998).
[3] A. P. Malanoski and P. A. Monson. J. Chem. Phys. **110,** 664 (1999).

[4] W. G. Hoover, N. E. Hoover, and K. Hanson. J. Chem. Phys **70,** 1873 (1979).
[5] S. C. Gay, J. C. Rainwater, and P. D. Beale. J. Chem. Phys. **112,** 9841 (2000).
[6] J. C. Rainwater. Int. J. Thermophys. **19,** 1523 (1998).
[7] S. Sastry, T. M. Truskett, P. G. Debenedetti, S. Torquato, F. H. Stillinger. **95,** 289 (1998).
[8] M. T. Lusk and P. D. Beale. Submitted to Phys. Rev. E.
[9] C. Vega, E. P. A. Paras, and P. A. Monson. J. Chem. Phys. **96,** 9060 (1992).